Neuroscience 195 (2011) 191–200

CYTOARCHITECTURAL DISRUPTION OF THE SUPERIOR COLLICULUS AND AN ENLARGED ACOUSTIC STARTLE RESPONSE IN THE *Tuba1a* MUTANT MOUSE

A. EDWARDS,[a] C. D. TREIBER,[b] M. BREUSS,[b] R. PIDSLEY,[a] G.-J. HUANG,[a] J. CLEAK,[a] P. L. OLIVER,[c] J. FLINT[a] AND D. A. KEAYS[c]*

[a]*Wellcome Trust Centre for Human Genetics, University of Oxford, Oxford, OX3 7BN, UK*

[b]*Institute of Molecular Pathology, Dr. Bohr-Gasse 1030, Vienna, Austria*

[c]*Medical Research Council, Functional Genomics Unit, Department of Physiology, Anatomy and Genetics, University of Oxford, South Parks Road, Oxford, OX1 3QX, UK*

Abstract—The *Jenna* mutant mouse harbours an S140G mutation in Tuba1a that impairs tubulin heterodimer formation resulting in defective neuronal migration during development. The consequence of decreased neuronal motility is a fractured pyramidal cell layer in the hippocampus and wave-like perturbations in the cerebral cortex. Here, we extend our characterisation of this mouse investigating the laminar architecture of the superior colliculus (SC). Our results reveal that the structure of the SC in mutant animals is intact; however, it is significantly thinner with an apparent fusion of the intermediate grey and white layers. Birthdate labelling at E12.5 and E13.5 showed that the S140G mutation impairs the radial migration of neurons in the SC. A quantitative assessment of neuronal number in adulthood reveals a massive reduction in postmitotic neurons in mutant animals, which we attribute to increased apoptotic cell death. Consistent with the role of the SC in modulating sensorimotor gating, and the circuitry that modulates this behaviour, we find that *Jenna* mutants exhibit an exaggerated acoustic startle response. Our results highlight the importance of *Tuba1a* for correct neuronal migration and implicate postnatal apoptotic cell death in the pathophysiological mechanisms underlying the tubulinopathies.

Key words: tubulin lissencephaly, superior colliculus, acoustic startle response.

The *Jenna* (*Jna*/+) mouse, generated from an *N*-ethyl-*N*-nitrosourea mutagenesis screen, has a dominantly inherited mutation in exon four of the α-tubulin gene, *Tuba1a* (Keays et al., 2007). This mutation, an S140G substitution, impairs tubulin heterodimer formation, which results in defects in neuronal migration during development. Consequently, mutant animals have a fractured pyramidal cell layer in the hippocampus, and laminar abnormalities in the cerebral cortex, predominantly in layers III and IV. Human studies have found that this mouse is a model for lissencephaly, a disorder characterised by simplified gyration of the cortex, mental retardation and epilepsy (Guerrini and Marini, 2006). Mutations in a number of genes cause lissencephaly, including DCX, LIS1, VLDLR and the *reelin* gene (des Portes et al., 1998; Gleeson et al., 1998; Hong et al., 2000; Boycott et al., 2005). In the later case, homozygous mutations in reelin result in gyral simplification, a thickened cortex and cerebellar hypoplasia (Hong et al., 2000).

Reelin, a large extracellular protein, was first implicated in neuronal migration after the identification of deletions in the *reeler* mouse, which is noted for its inverted cortex and disorganised hippocampus and cerebellum (D'Arcangelo et al., 1995). More recently, the catalogue of neuroanatomical abnormalities in the *reeler* mouse has been extended to the superior colliculus (SC). In vertebrates, the SC consists of seven layers that are both anatomically and functionally organised. The superficial SC consists of the three uppermost layers: the zonal (Zn), superficial grey (SuG) and the optic layer (Op), and the deep SC contains four layers: the intermediate grey (InG), intermediate white (InW), deep grey (DpG) and deep white (DpW). In the reeler mouse, it has been reported that the superficial layers of this structure are cytoarchitectually and myeloarchitectually disorganised (Baba et al., 2007). Similarly, disruption of the laminar patterning in the SC has been observed in the *reelin*-deficient shaking rat Kawasaki (Sakakibara et al., 2003).

Given that both mutations in reelin and TUBA1A cause similar phenotypes in humans, in this article, we set out to investigate the cytoarchitecture of the SC in the *Jna*/+ mice. Using histological tools, we found that the laminar structure of the SC in mutant animals was intact; however, it was significantly thinner with an apparent fusion of the InG and InW. Using birthdate labelling, we showed that the neuronal migration defect that is observable in the cortex and the hippocampus of affected animals is also apparent during the formation of the SC. Additionally, an elevated rate of cell death leads to a significant loss of neurons in the SC of the *Jna*/+ mouse between postnatal day 21 (P21) and 12 weeks of age, with the majority of the loss occurring in the deep layers. Consistent with the role of the SC in modulating sensorimotor gating, we observed an

*Corresponding author. Tel: +43-1-797-30-3530; fax: +43-1-798-71-53.
E-mail address: keays@imp.ac.at (D. A. Keays).

Abbreviations: BrdU, 5-bromo-2-deoxyuridine; DAPI, 4',6-diamidino-2-phenylindole; DpG, deep grey layer; DpW, deep white layer; InG, intermediate grey layer; InW, intermediate white layer; *Jenna*, *Jna*/+; Op, optic layer; PAG, periaqueductal grey; SC, superior colliculus; SuG, superficial grey layer; Tpd52L1, tumour protein D52-like-1; Zn, zonal layer.

0306-4522/11 $ - see front matter
doi:10.1016/j.neuroscience.2011.08.035

exaggeration of the acoustic startle response in mutant animals.

EXPERIMENTAL PROCEDURES

Animals

Mice were maintained on a C3H/HeH (Harlan, UK) background and housed on a 12:12 light:dark cycle at a temperature of 22±1 °C and humidity of 60%–70%. Males and females were separated at weaning (P21) and housed separately in groups of five where possible. The genotype of animals was determined by polymerase chain reaction analysis, as previously described (Keays et al., 2007), and only littermates were selected for experiments. Cages were environmentally enriched with cardboard tubing, and mice were permitted *ad libitum* access to food. Experiments were performed in accordance with the UK Animals (Scientific Procedures) Act 1986.

5-bromo-2-deoxyuridine (BrdU) labelling

For birthdate labelling experiments, pregnant C3H females were injected with BrdU (50 μg/g of body weight), 12.5 and 13.5 days after copulation. All resultant P0 pups were killed and genotyped. P0 brains were extracted and drop-fixed in 4% paraformaldehyde for 4 h before being placed in sucrose overnight. Brains were then embedded in OCT and sectioned at 14 μm using a cryostat, then mounted onto electrostatic slides and stored at −20 °C. Prior to staining, antigen retrieval was performed in citrate buffer at 90 °C (0.01 M, pH 6). To quench peroxidase activity, slides were placed in 3% H_2O_2 solution for 10 min, followed by three washes in PBS. Sections were then digested in trypsin (0.0125%) for 10 min at 37 °C, washed three times in PBS, followed by a 20-min incubation in 2 N HCl at 37 °C. After washing, slides were incubated in a 0.3% Triton/PBS with 2% rabbit serum (Rat Elite ABC Kit, Vector Labs, Peterborough, UK) and 1:100 rat anti-human BrdU antibody (Accurate Chemical & Scientific, Westbury, NY, USA) in a humidity chamber overnight. Slides were then washed and stained as directed in the Elite ABC Kit, using DAB permanent staining.

Gallyas staining

Twelve-week-old *Jna*/+ mice and wild-type (WT) littermates were perfused with 0.9% saline and 10% formalin solution. Brains were extracted and left in 10% formalin solution for 2 weeks. Subsequently, brains were cryoprotected in 30% sucrose/formalin and sectioned on a freezing microtome (25 μm) before storing in 5% formalin solution at 4 °C for a further 2 weeks. Sections were matched, mounted on electrostatically charged slides and stained using a Gallyas silver staining method based on study by Pistorio et al. (2006).

In situ hybridisation

A 429-base pair probe targeting the tumour protein D52-like-1 (Tpd52L1) gene was generated by PCR using the following primers: Tpd521l_F GAAAGTAGGTGGGACAAACCAC and Tpd521l_R GGAGACCAAGTCAAAACCAAAG and cloned into a pCR2.1-TOPO vector (Invitrogen, CA, USA). Digoxigenin-labelled riboprobes were then synthesized using appropriate RNA polymerases (Roche Applied Science, Burgess Hill, UK), and hybridisation was performed, as previously described (Isaacs et al., 2003). All hybridisations were performed on 14-μm brain sections prepared from *Jna*/+ mice and WT littermates aged 12 weeks.

Juvenile and adult immunohistochemistry

Cohorts of P21 and 12-week-old *Jna*/+ and WT littermate mice (n=4) were perfused with 0.9% NaCl and 4% paraformaldehyde, and brains were postfixed for 6 h, followed by dehydration in 30% sucrose solution. Sections (40 μm) were prepared on a freezing microtome and stored in antifreeze solution at −20 °C. For each P21 and 12 week brain, three matched SC sections were selected for staining. Sections were incubated with the primary antibody overnight in 0.3% Triton/PBS with 2% of the appropriate serum at the following concentrations: NeuN (1:500) (Millipore, Billerica, MA, USA); Calbindin (1:500) (Millipore, Billerica, MA, USA); Er81 (1:4000). After three washes in PBS (5 min each), sections were incubated with a biotinylated secondary antibody (1:500) in 0.3% Triton/PBS for 2 h. After a series of washes in PBS, sections were incubated for 1 h with fluorescein-conjugated streptavidin (1:500) (Vector Labs, Peterborough, UK). Sections were mounted on electrostatic slides andcoverslipped with 4',6-diamidino-2-phenylindole (DAPI) containing mounting media (Vector Labs, Peterborough, UK).

Apoptosis study

Seven-week-old mice *Jna*/+ and WT littermate mice were perfused and sectioned in the aforementioned manner (n=5). Every 8th section from the beginning of the SC through to the start of the inferior colliculus was mounted on electrostatic slides. Prior to staining, slides underwent antigen retrieval, peroxidase quenching and PBS washing. Sections were incubated with the caspase 3 primary antibody (1:400) (Cell Signaling Technology, Boston, MA, USA) overnight in 0.3% Triton/PBS with 2% goat serum. Slides were then washed and stained, as directed in the Elite ABC Kit, using DAB permanent staining. Total cell counts were then obtained by multiplying the number of positive cells observed by a factor of 8.

Quantification and statistics

The SC was analysed through the creation of 10 zonal analysis boxes in which cells could be counted. Boxes were drawn on SC images using ImageJ freeware, were positioned 100 μm from the midline and were a consistent 250 μm in width. The boxes were of equal height within an image, with the height of each box being a 10th of the distance between the surface of the Zn to a depth in the periaqueductal grey (PAG) level with the cerebellar aqueduct. Once the analysis boxes were formatted, labelled cells within each box were counted manually. The percentage of neurons within each box was calculated from the number of NeuN staining cells as a proportion of DAPI cells. Statistics were performed in GraphPad Prism. A 1-way ANOVA with a Bonferroni correction for multiple comparisons was used for the analysis of behavioural measurements and for NeuN, BrdU and DAPI cell density zonal measurements.

Behavioural testing

The acoustic startle response was measured using a commercially available behavioural testing system (San Diego Instruments, San Diego, CA, USA). This apparatus consisted of a sound-proof box with a 6-cm speaker to deliver the acoustic stimuli, coupled to an accelerometer to monitor the animal's movement. The behavioural testing was performed in a separate room, and the cages were moved into the room at least 2 h before the start of the experiment. Prior to testing, each mouse was placed inside the startle apparatus and allowed to acclimatise for 5 min. To test the acoustic startle response, acoustic stimuli were presented as 40-ms impulses of white noise with four different intensities (90, 100, 110 and 120 dB) for a total of 20 times, each in a pseudorandom order and spaced at random intervals between 10 and 20 s. Responses were expressed in arbitrary units and averaged for each type of trial.

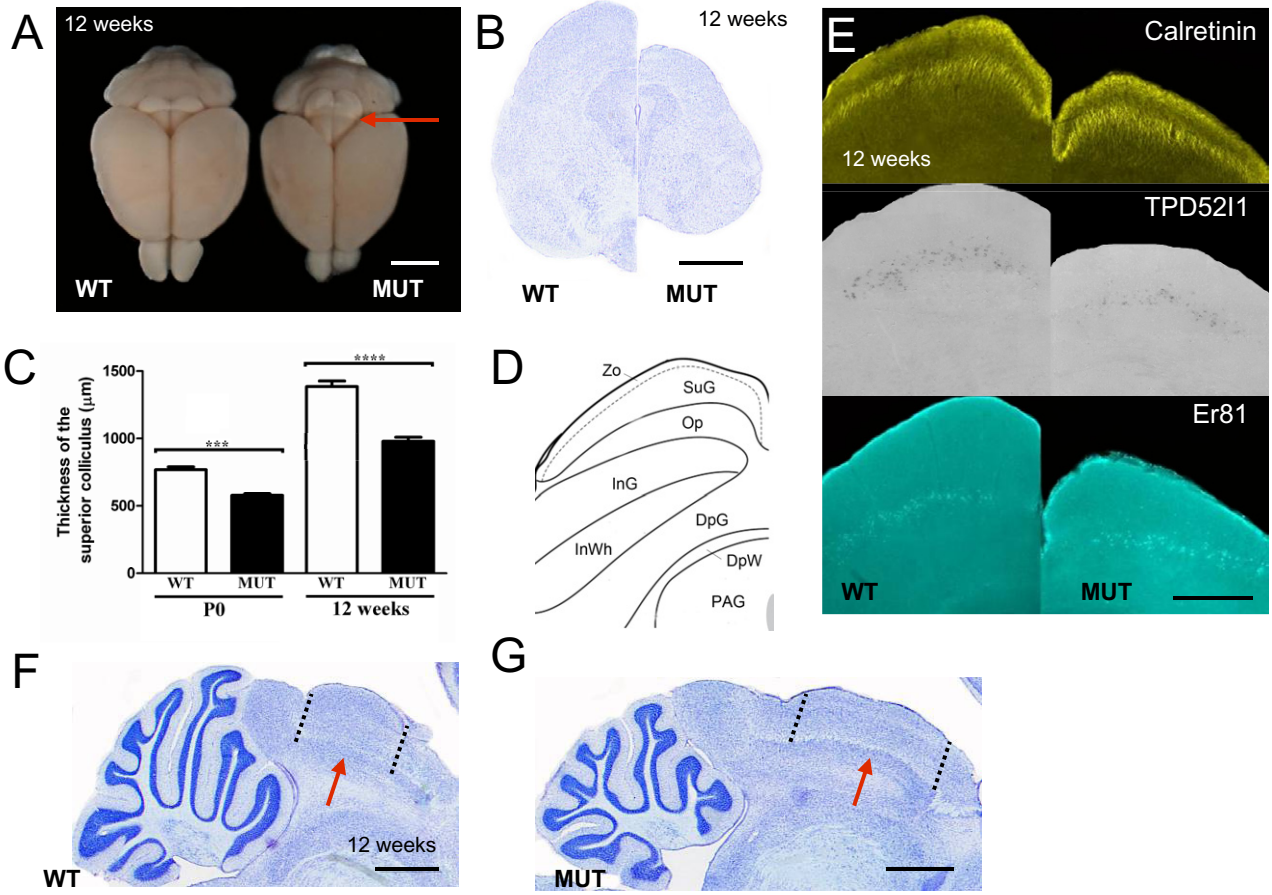

Fig. 1. The structure of the SC in *Jnal*+ mutants. (A) Dorsal view of wild-type (WT) and *Jnal*+ brains. The red arrow highlights the exposed SC in mutant animals. (B) Coronal Nissl stain of WT and mutant animals illustrating the thinner SC in *Jnal*+ mutants. (C) Quantification of the thickness of the SC in WT and mutant animals at P0 and 12 wk reveals a significant difference between controls and *Jnal*+ animals ($F=18.1$, $P<0.001$, $F=102.4$, $P<0.0001$). (D) Diagram illustrating the laminar structure of the SC adapted from Paxinos and Watson's Brain Atlas (Paxinos et al., 2007). The SC consists of seven layers: the zonal layer (Zn), the superficial grey layer (SuG), the optic layer (Op), the intermediate grey layer (InG), the intermediate white layer (InW), the deep grey layer (DpG) and the deep white (DpW) layer. Other abbreviation: PAG, periaqueductal grey. (E) Calretinin, TPD52I1 and ER81 staining (top to bottom) reveal that the laminar structure of the SC is intact in *Jnal*+ mutants. (F, G) Sagittal sections of the SC in WT littermates and mutant animals reveal that it is elongated in *Jnal*+ mutants (G). Red arrow between dotted black lines shows the SC. Scale bars 5 mm (A), 1 mm (B, F, G) and 250 μm (E).

RESULTS

Structure of the SC in the *Jnal*+ mouse

When dissecting brains from adult *Jnal*+ mutants, it is immediately apparent that the SC is more exposed in comparison to control animals (Fig. 1A). A sagittal Nissl stain reveals that it is also elongated in the rostrocaudal plane in comparison with WT controls (Figs. 1F, G), and a coronal Nissl stain (Fig. 1B) demonstrates that it is thinner both at P0 ($F=18.16$, $P<0.001$) and 12 weeks of age ($F=102.41$, $P<0.0001$) (Fig. 1C). To investigate the laminar structure of the SC, we began by searching for markers that selectively label different cellular populations. We tested commonly used cortical makers (Cux-1, Foxp2, ER81, calbindin, calretinin) and searched the Allen Brain Atlas for genes that showed layer-specific expression (Lein et al., 2007). We found that calretinin, which labels GABAergic interneurons in layers 2/3 of the mouse cortex labels the superficial OP layers (Park et al., 2002); TPD52L1, a cell cycle-regulated protein labels cells in the proximity of the InG (Boutros and Byrne, 2005) and Er81, a transcription factor which labels layer V neurons in the cortex, localised slightly deeper to InG/InW (Watakabe et al., 2007). Nissl staining, immunohistochemistry (Er81 and calretinin) and *in situ* hybridisation (TPD52L1) revealed that, despite some dispersion of Er81 and calbindin-positive cells, the laminar structure of the SC in *Jnal*+ mutants is essentially intact (Fig. 1E). Next, we used a Gallyas silver stain to investigate the myeloarchitecture of the colliculus (Gallyas, 1979) (Fig. 2A). In WT animals, a clear distinction could be made between the various grey and white layers, the dark silver stain labelling the white matter, particularly the Op layer, and the large myelinated cells in the InW (Fig. 2C). In mutants, the definition between superficial and intermediate layers was less defined, exemplified by the fusion of the InG layer with the InW layers (Fig. 2D). The SC commissure that is observable in the DpW was observed to cross the midline in both WT controls and *Jnal*+ mutants (Figs. 2E, F).

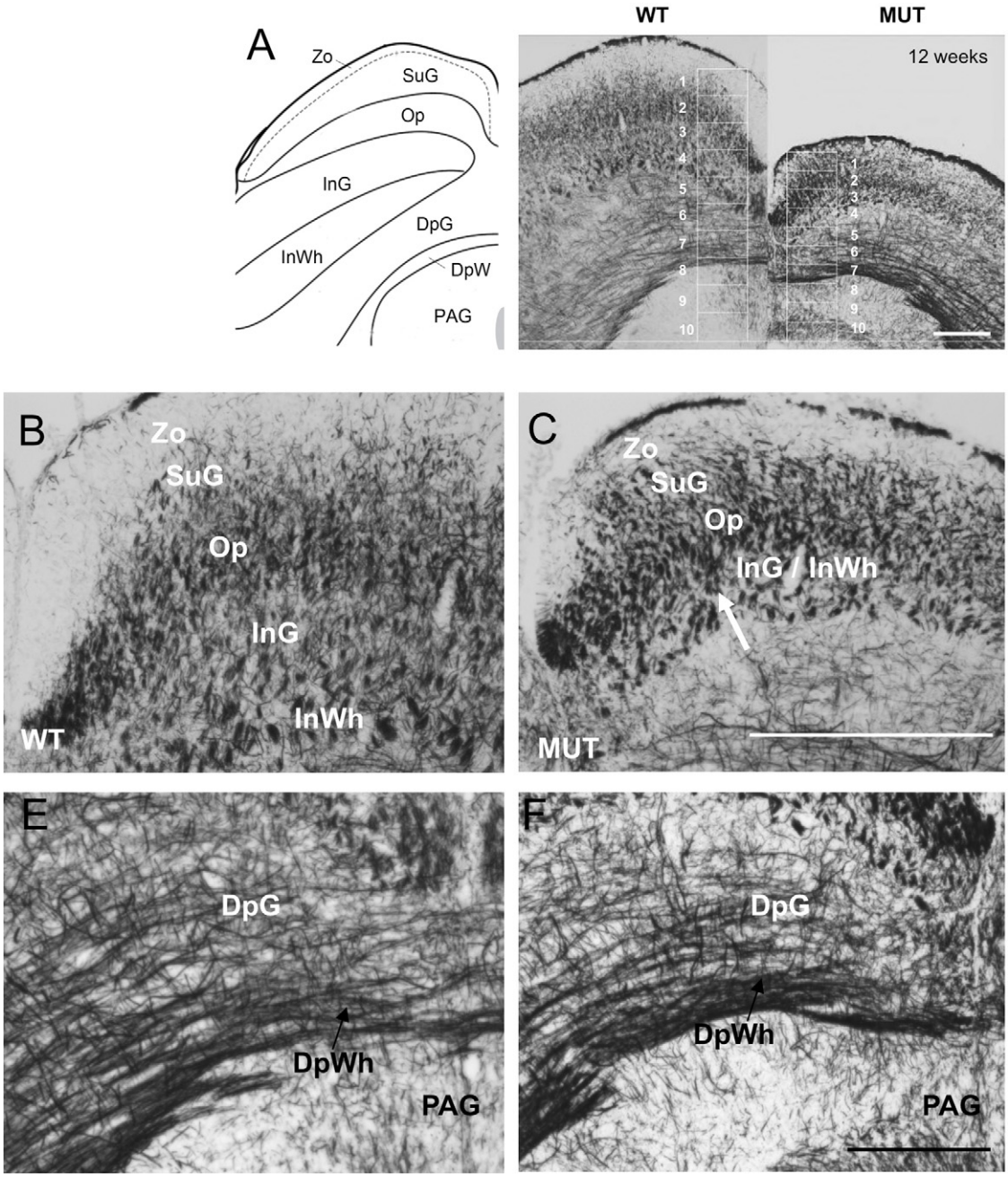

Fig. 2. Myeloarchitectural investigation of the SC in *Jnal*+ mutants. (A) Diagram illustrating the laminar structure of the SC adapted from Paxinos and Watson's Brain Atlas (Paxinos et al., 2007). (B) Diagram showing the layers of the SC aligned with Gallyas-stained WT and mutant sections. Equally proportioned analysis boxes (shown in white) were drawn from the aqueduct to the dorsal surface of Zn layer. These boxes map to similar anatomical regions. Boxes 1–5 align with the superficial and intermediate layers (Zn, SuG, Op InG, InW), Boxes 6, 7 the deep layers (DpG, DpW) and Boxes 8–10 the PAG. (C, D) Enlarged images of the superficial and intermediate layers of Gallyas-stained sections in WT and mutant animals. The superficial SC of the mutant appears compacted and less defined with a fusion of the InG and InW (white arrow). (E, F) Enlarged images of the deep layers (DpG and DpW) of Gallyas-stained sections in WT and mutant animals. Sections appear similar, with crossing of the collicular commissure observed in both mutants and WT animals. Scale bars show 250 μm.

Defective neuronal migration in the *Jnal*+ SC

We then examined whether the anatomical abnormalities observed in the SC might be associated with a defect in neuronal migration. The laminar structure of the SC differs from the neocortex, as most GABAergic interneurons migrate radially, and there is a temporal overlap in neurogenesis between deep and superficial layer neurons (Tan et al., 2002; Tsunekawa et al., 2005). The peak generation time for deep layer neurons (which migrate in an inside-out manner) is E11 to E13, and for superficial layer neurons (which migrate in a more complex pattern) is E12 to E13 (Altman and Bayer, 1981; Edwards et al., 1986). We la-

belled newly born cells with BrdU at E12.5 and E13.5. Harvesting mice at their day of birth, we counted labelled cells, having divided the SC into 10 equal zones extending from the aqueduct to the surface of the colliculus (Figs. 3A, B). We tested for an interaction between genotype and the mean percentage of cells in each zone. When labelling at E12.5, we found that the percentage of labelled cells present in the two most superficial analysis boxes was significantly reduced in *Jna*/+ mutants (n=4) (F=20.3, P< 0.0001; F=26.96, P<0.0001 [zones 1 and 2, respectively]). This was complemented by a significantly higher percentage of BrdU-labelled cells present in zone 6 (a region that includes the DpG) in *Jna*/+ mutants (F=11.78, P<0.01) (Figs. 3A, E). When labelling at E13.5, which labels a higher percentage of superficial neurons, we found a significant reduction in the portions of BrdU-labelled cells in zones 2 (F=10.56, P<0.05) and 3 (F=18.32, P<0.001) and a higher portion in zones 6 (F= 20.9, P<0.0001) and 7 (F=15.39, P<0.01) in *Jna*/+ animals (n=3) (Figs. 3B, F). These results are indicative of a defect in neuronal migration in *Jna*/+ mutants. Overall, we observed no significant difference in the total number of BrdU-labelled cells when comparing WT and *Jna*/+ mutants when labelling at E12.5 (F=0.56, P>0.5) or E13.5 (F=1.19, P>0.1) suggesting that the rate at which neurons are generated is not affected by the S140G mutation (Figs. 3C, D).

Next, we examined the distribution of neurons in the SC in juvenile animals by staining serial sections with the postmitotic marker NeuN at P21 (n=4), again dividing the SC into 10 zones. We tested for an interaction between genotype and the mean percentage of NeuN-positive cells in each zone. Although we observed a higher percentage of neurons in the deep layers in mutant animals, this difference was not significant (Fig. 3G). These results suggest that either the neurons delayed during development catch up between P0 and P21, or alternatively, the SC in mutant animals is remodelled by differential rates of apoptosis in the deep, intermediate and superficial zones (Finlay et al., 1982; Cowan et al., 1984).

Loss of neurons in the adult SC in *Jna*/+ mutants

Next, we assessed how the S140G mutation affects the survival of neurons within the layers of the SC at P21 and 12 weeks of age. We once again divided the colliculus into 10 equal bins extending from the aqueduct to the surface, and counted the number of NeuN-positive and DAPI-labelled cells (n=4) (Figs. 4A, B). At P21, we found that both mutant and littermate control animals had similar percentages of neurons (50%) in each zone (Fig. 4C). This contrasts with our observations at 12 weeks of age, where we found a large reduction in the percentage of neurons in all zones in mutant animals (Fig. 4D). The greatest loss of neurons occurred in zones 6 and 7 in the vicinity of the DpG and DpW (F=33.07, P<0.0001; F=41.57, P< 0.0001). Additionally, zones 8–10, which cover the PAG showed a significant drop in the percentage of neurons (F=32.58, P<0.0001; F=18.87, P<0.001; F=28.2, P< 0.0001). To demonstrate that this loss of neurons is due to cell death, we immunostained coronal sections of the SC with an antibody specific for caspase-3, an activated protease that labels apoptotic cells (Porter and Janicke, 1999). We performed this experiment on mice aged 7 weeks of age (n=5), a time point midway between P21 and 12 weeks (Figs. 4E, F). Staining of serial sections revealed that there was a significant increase in both the number (F=21.2, P<0.01) and density (F=72.1, P<0.0001) of caspase-3-positive cells in *Jna*/+ mutants (Figs. 4G, H).

Exaggerated acoustic startle response in *Jna*/+ mutants

Inhibitory cells in the deep layers of the SC have been implicated in mediation of the acoustic startle response (Meloni and Davis, 2000), a behaviour that is characterised by the involuntary contraction of muscles in response to a sudden acoustic stimulus (Koch, 1999). Therefore, we tested the acoustic startle response in *Jna*/+ mutants by exposing them to 40-ms impulses of white noise with four different intensities (90, 100, 110 and 120 dB) in a pseudorandom order and spaced at random intervals between 10 and 20 s. We found that in the absence of a weight correction, the acoustic startle response is significantly higher in both males and female *Jna*/+ mutants when exposed to a 120 dB stimulus (male [F=56.1, P<0.0001], female [F=48.08, P<0.0001]) (Figs. 5A, B). When normalising for the reduced mass of *Jna*/+ mutants, we found that mutant animals of both sexes display a significantly larger acoustic startle response to both 110 dB (male [F=17.85, P<0.001], female [F=15.5, P<0.001]) and 120 dB stimuli (male [F=134.8, P<0.0001], female [F=96.8, P<0.0001]) (Figs. 5C, D).

DISCUSSION

In this article, we have shown that the S140G mutation in *Tuba1a* mutant animals results in a cytoarchitecturally disrupted SC. Although the general lamination of the SC is intact, our studies have revealed a marked thinning of the SC, with a fusion of the InG layer with the InW layers. Birthdate labelling at E12.5 and E13.5, followed by examination at P0, revealed a severe impairment in the radial migration of neurons. Cell counting using the neuronal marker NeuN demonstrated that the distribution of neurons at P21 in mutant animals was comparable with WT controls suggesting postnatal rectification of migration, or alternatively, remodelling of the SC coincident with axonal innervation (Finlay et al., 1982; Cowan et al., 1984). A quantitative assessment of neuronal number in adulthood showed that there was a massive reduction in the percentage of postmitotic neurons in mutant animals, which we attribute to an increase in neuronal apoptosis between P21 and 12 weeks of age in *Jna*/+ mutants. Consistent with the role of the SC in modulating sensorimotor gating, and the circuitry that modulates this behaviour, we find that *Jna*/+ mutants exhibit an exaggerated acoustic startle response.

What underlying cellular defect might cause these phenotypes? Our results suggest that the thinning of the SC, as well as the reduction of neurons in adulthood, is unlikely

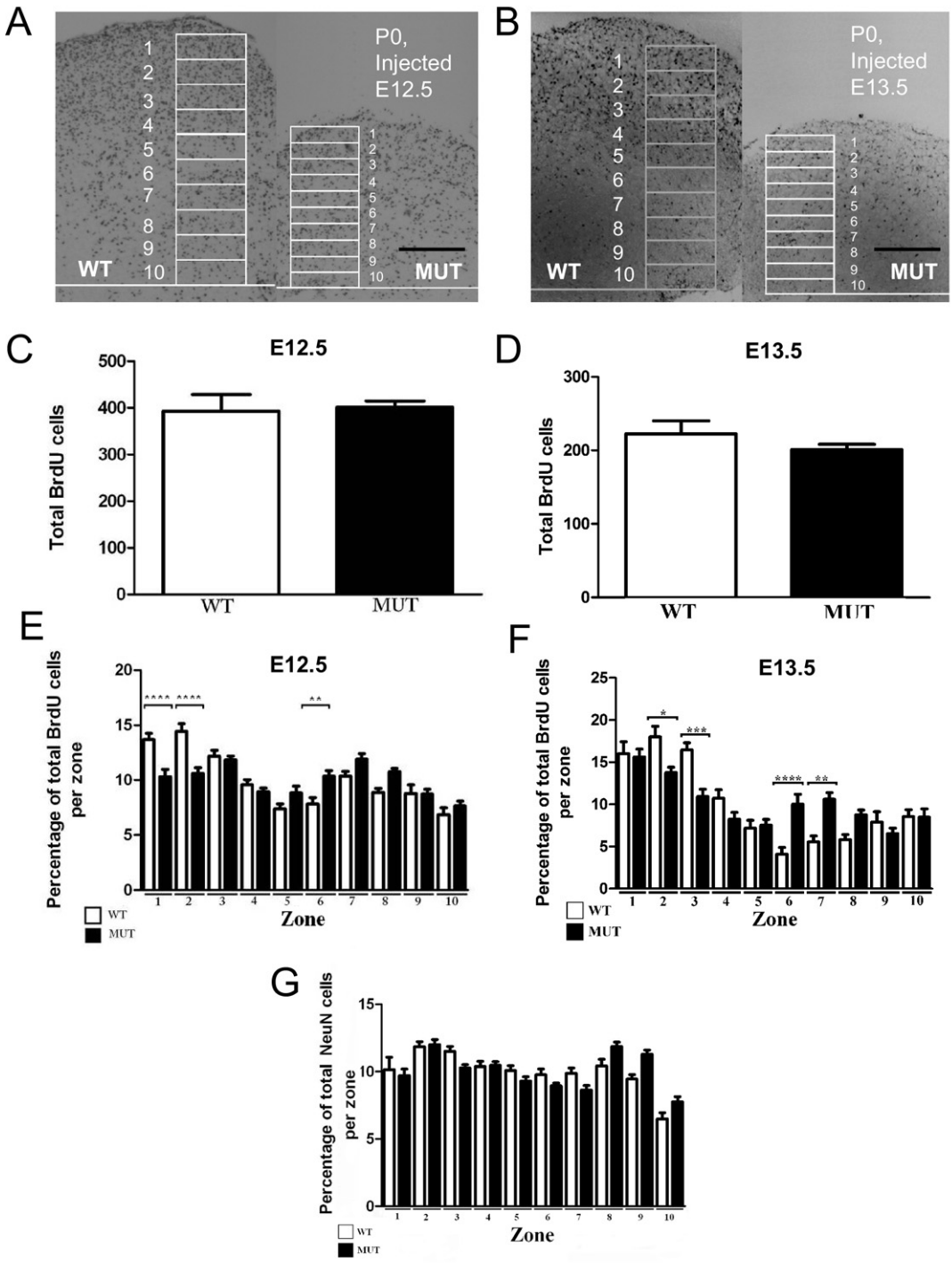

Fig. 3. Impaired neuronal migration in the SC of *Jnal*+ mutants. (A, B) Staining for BrdU in the SC of littermate controls and *Jnal*+ mutants harvested at P0 after injection of BrdU at E12.5 (n=4) and E13.5 (n=3). The SC was divided into 10 equal bins (shown in white) extending from the aqueduct to the dorsal surface of Zn layer and BrdU-positive cells were counted. (C, D) There was no significant difference in the average number of cells labelled per section between WT littermates and *Jnal*+ mutants. (E, F) The distribution of BrdU-positive cells per zone in WT controls and *Jnal*+ mutants after injections at E12.5 (E) and E13.5 (F). The percentage of BrdU cells in the upper two zones was significantly reduced in *Jnal*+ mutants when injected at E12.5 (layer 1 [F=20.3, P<0.001], layer 2 [F=27, P<0.001]), and higher in layer 6 (F=11.78, P<0.01). Similarly, when injected at E13.5, the percent of BrdU-labelled cells in zones 2 (F=10.56, P<0.05) and 3 (F=18.32, P<0.001) was reduced in *Jnal*+ animals (n=3), complemented by a higher portion observed in zones 6 (F=20.9, P<0.0001) and 7 (F=15.39, P<0.01) (n=3). (G) Staining of postmitotic neurons with the marker NeuN reveals no significant difference in the percentage of neurons per a zone at P21. Scale bars in A and B show 250 μm.

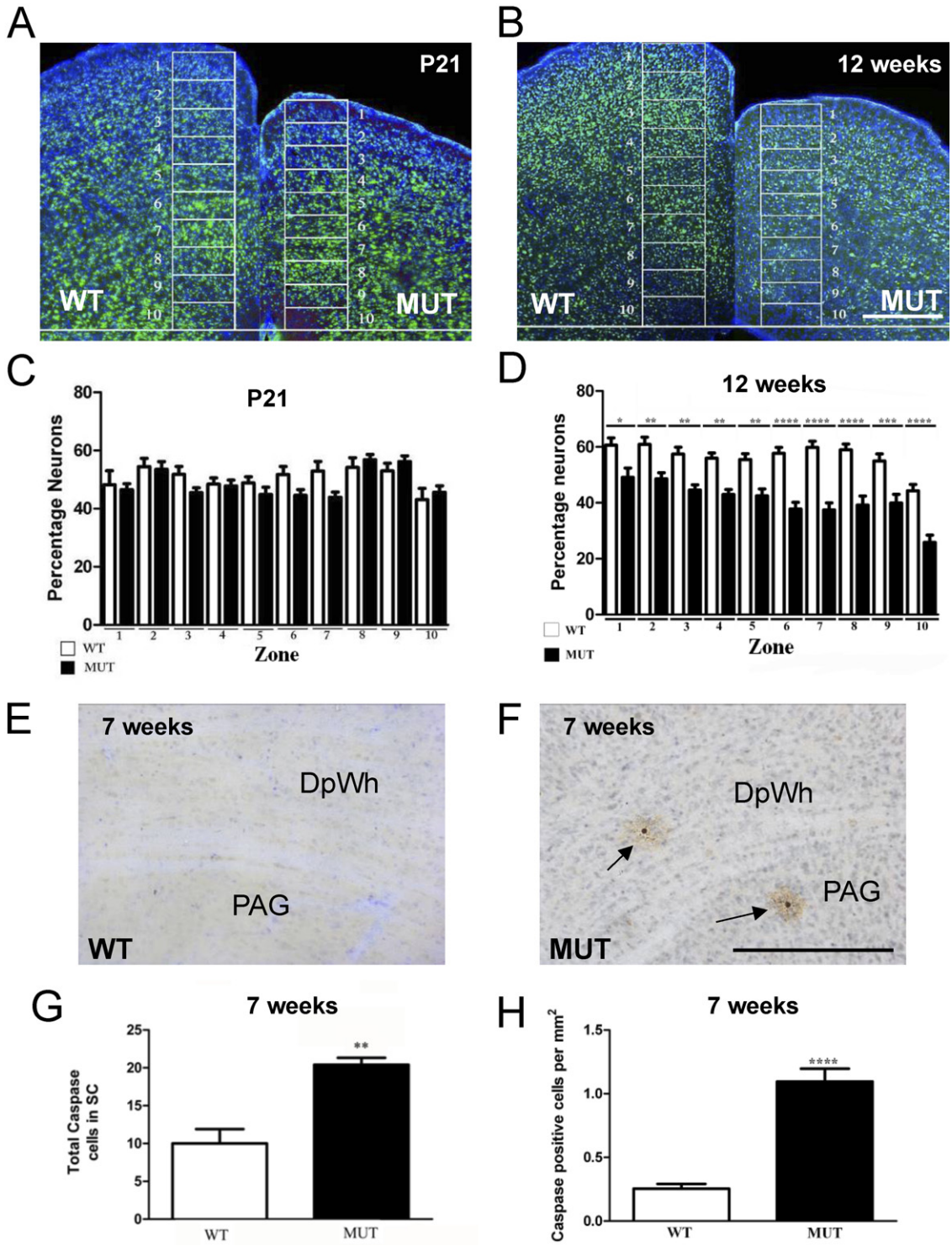

Fig. 4. Loss of neurons and increased apoptosis in the SC of *Jna*/+ mutants. (A, B) The SC was divided into 10 equal bins and DAPI (blue) and NeuN (green)-labelled cells counted at P21 and 12 wk of age for both WT littermates and *Jna*/+ mutants (n=4). This enabled the percentage of neurons to be calculated for each zone at each time point (C, D). We compared the percentage of neurons in WT littermates and *Jna*/+ mutants and found no significant difference between genotypes for any zone in the P21 cohort (C). In contrast, there was a massive reduction in the percentage of neurons throughout the SC in 12-wk-old *Jna*/+ mutants (D). The loss of neurons reached significance in all zonal boxes, particularly those mapping to the DpG/DpW layers (zone 6 [F=33.07, P<0.001], zone 7 [F=41.57, P<0.001]). (E, F) Immunostaining of the SC of 7-wk-old animals revealed a significant increase in the total number (F=21.2, P<0.01) and density (F=72.1, P<0.0001) of caspase-positive cells (black arrows) in *Jna*/+ mutants (n=5) when compared with WT littermates (G, H). Scale bars show 250 μm.

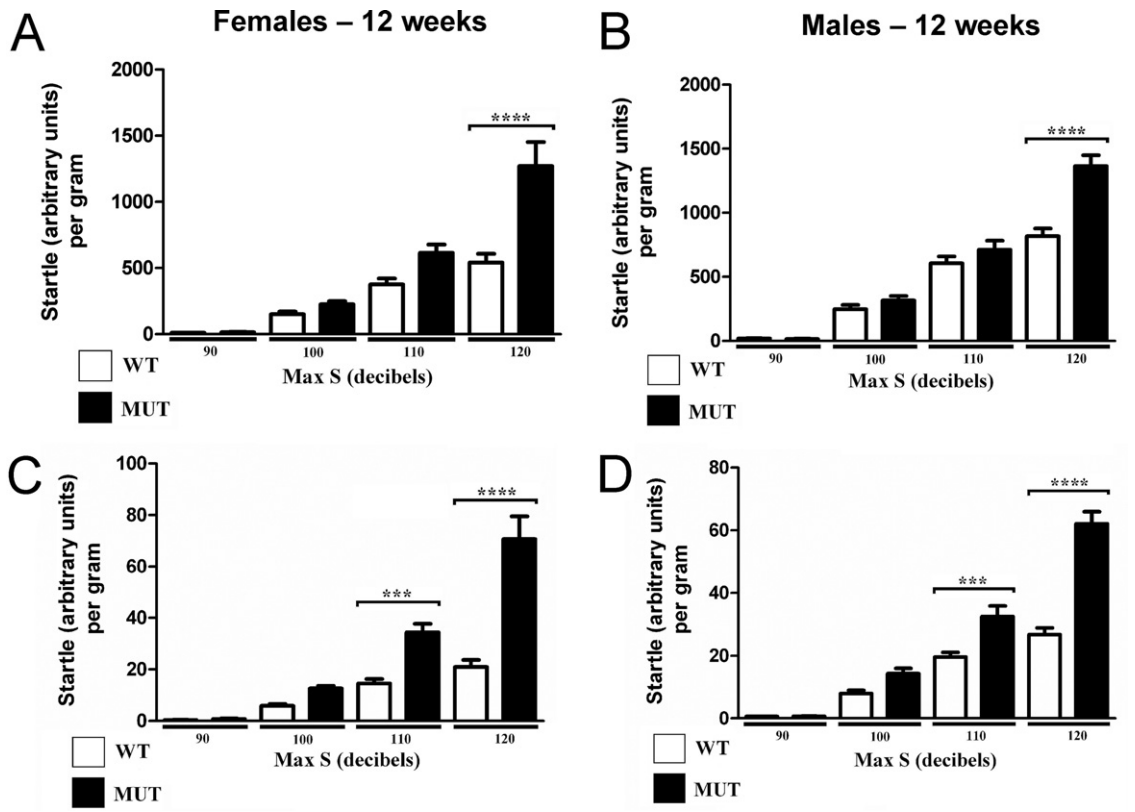

Fig. 5. Exaggerated acoustic startle response in *Jnal*+ mutants. (A, B) Assessment of the acoustic startle response in male (n=7) and female *Jnal*+ mutants (n=8) in response to randomised 40 ms bursts of 90 dB, 100 db, 110 db and 120 db white noise. In the absence of a weight correction, the acoustic startle response is significantly higher in both males and female *Jnal*+ mutants when exposed to a 120 dB stimulus (male [F=56.1, P<0.0001], female [F=48.08, P<0.0001]). (C, D) When these data are normalised to take into account the differences in weight between genotypes, mutant animals of both sexes display a significantly larger acoustic startle response to 110 dB (male [F=17.85, P<0.001], female [F=15.5, P<0.001]) and 120 dB stimuli (male [F=134.8, P<0.0001], female [F=96.8, P<0.0001]).

to be a result of a defect in mitotic division. We observe comparable numbers of labelled cells in WT controls and *Jnal*+ mutants after injections of BrdU at E12.5 and E13.5, and all currently available evidence suggests that *Tuba1a* is limited in its expression to postmitotic neurons (Bamji and Miller, 1996; Gloster et al., 1999; Keays et al., 2010). Instead, we implicate increased cell death in the pathophysiology of the tubulinopathies showing a massive increase in apoptosis in the adult SC in *Jnal*+ mutants. Our mouse data are consistent with observations made in human patients with mutations in TUBA1A. Bahi-Buisson and colleagues have reported five patients with mutations in TUBA1A who presented with severe microcephaly (R264C, L397P, R422C, G436R, R422H) despite normal biparietal diameters in the third trimester (Bahi-Buisson et al., 2008), and Morris-Rosendahl and colleagues have identified two patients with mutations in TUBA1A (R402L, E55K) who again exhibit progressive microcephaly (Morris-Rosendahl et al., 2008). Taken together with our mouse data, we conclude that mutations in *Tuba1a* can lead to an increase in neuronal apoptosis.

How might a mutation in *Tuba1a* cause an increase in neuronal apoptosis? The molecular cascade that regulates cell death involves a host of proteins that include members of the caspase family, Fas, Bcl, Pten and Bax (Merry et al., 1994; Vekrellis et al., 1997; Cheema et al., 1999; Groszer et al., 2006). An attractive candidate for mediation of apoptosis in the *Tuba1a* mutant mice is the GTPase, RhoA. RhoA, along with a host of other small GTP-binding proteins that include Rnd2, Rac1 and Cdc42, acts within multiple signalling pathways that converge on the actin and microtubule cytoskeletons to regulate neuronal morphology, adhesion and migration (Luo, 2000; Govek et al., 2005). Tucker and colleagues have extended the functional repertoire of RhoA, recently implicating it in the control of postnatal apoptosis in the vertebrate brain (Sanno et al., 2010). Using a dominant-negative genetic inhibitor of the Rho GTPases, they showed that inhibition of Rho GTPases results in a large increase in the number and density of neurons in the somatosensory cortex of mice, a consequence of decreased apoptosis. Cellular studies attributed this affect to RhoA, which was found to cause increased apoptosis when overexpressed in cultured cortical neurons. Sitting at a molecular intersection between the cytoskeleton and an apoptotic signalling pathway, it is possible that in response to microtubule dysfunction, activated RhoA may mediate programmed cell death in *Jnal*+ mutants (Wittmann and Waterman-Storer, 2001).

We have shown that the loss of neurons, as well as the cytoarchitectural abnormalities apparent in the SC, is ac-

companied by an increase in the acoustic startle response in *Jnal*/+ mutant mice. The acoustic startle response is mediated by a well-characterised circuit that consists of the auditory nerve, the ventral cochlear nucleus, the dorsal nucleus of the lateral lemniscus, the caudal pontine reticular nucleus, spinal interneurons and spinal motor neurons (Davis et al., 1982; Koch, 1999). Neurons located deep in the SC, where we observe the greatest loss of neurons in *Jnal*/+ mutants, receive GABAnergic input from the substantia nigra and synapse directly with those in the caudal pontine reticular nucleus modulating the startle response (Shammah-Lagnado et al., 1987; Meloni and Davis, 1999, 2000). Although we cannot exclude the presence of anatomical or functional defects associated with other elements of this circuit, the cell loss and cytoarchitectural disruption of the SC we observe in the *Jnal*/+ mouse are consistent with the abnormal acoustic startle response we have described in this article.

This study has shown that the S140G mutation in the *Jnal*/+ mouse results in an impairment of neuronal migration in the developing SC, an increase in adult neuronal apoptosis and an enlarged acoustic startle response. These observations raise several interesting questions. First, it provides additional evidence for the importance of *Tubala1a* for neuronal migration, prompting the question: is *Tuba1a* vital for all forms of neuronal migration? Might *Tuba1a* also be required for the correct migration of peripheral neurons and those that form the precise lamination in the retina? Second, is the increased neuronal apoptosis we observe in the SC, a more global phenomenon? Might we also observe increased cell death in the adult telencephalon in *Jnal*/+ mutants? Third, one is compelled to ask whether the acoustic startle response and SC are also abnormal in human patients who harbour mutations in *Tuba1a*?

Acknowledgments—We are grateful to Dr. Thomas Jessel for his gift of ER81 antibody. This work is supported by a grant from Le Fondation Jérôme Lejeune and the Wellcome Trust. DAK is supported by an FWF grant (P21092).

REFERENCES

Altman J, Bayer SA (1981) Time of origin of neurons of the rat superior colliculus in relation to other components of the visual and visuomotor pathways. Exp Brain Res 42:424–434.

Baba K, Sakakibara S, Setsu T, Terashima T (2007) The superficial layers of the superior colliculus are cytoarchitectually and myeloarchitectually disorganized in the reelin-deficient mouse, reeler. Brain Res 1140:205–215.

Bahi-Buisson N, Poirier K, Boddaert N, Saillour Y, Castelnau L, Philip N, Buyse G, Villard L, Joriot S, Marret S, Bourgeois M, Van Esch H, Lagae L, Amiel J, Hertz-Pannier L, Roubertie A, Rivier F, Pinard JM, Beldjord C, Chelly J (2008) Refinement of cortical dysgeneses spectrum associated with TUBA1A mutations. J Med Genet 45:647–653.

Bamji SX, Miller FD (1996) Comparison of the expression of a T alpha 1: nlacZ transgene and T alpha 1 alpha-tubulin mRNA in the mature central nervous system. J Comp Neurol 374:52–69.

Boutros R, Byrne JA (2005) D53 (TPD52L1) is a cell cycle-regulated protein maximally expressed at the G2-M transition in breast cancer cells. Exp Cell Res 310:152–165.

Boycott KM, Flavelle S, Bureau A, Glass HC, Fujiwara TM, Wirrell E, Davey K, Chudley AE, Scott JN, McLeod DR, Parboosingh JS (2005) Homozygous deletion of the very low density lipoprotein receptor gene causes autosomal recessive cerebellar hypoplasia with cerebral gyral simplification. Am J Hum Genet 77:477–483.

Cheema ZF, Wade SB, Sata M, Walsh K, Sohrabji F, Miranda RC (1999) Fas/Apo [apoptosis]-1 and associated proteins in the differentiating cerebral cortex: induction of caspase-dependent cell death and activation of NF-kappaB. J Neurosci 19:1754–1770.

Cowan WM, Fawcett JW, O'Leary DD, Stanfield BB (1984) Regressive events in neurogenesis. Science 225:1258–1265.

D'Arcangelo G, Miao GG, Chen SC, Soares HD, Morgan JI, Curran T (1995) A protein related to extracellular matrix proteins deleted in the mouse mutant reeler. Nature 374:719–723.

Davis M, Gendelman DS, Tischler MD, Gendelman PM (1982) A primary acoustic startle circuit: lesion and stimulation studies. J Neurosci 2:791–805.

des Portes V, Pinard JM, Billuart P, Vinet MC, Koulakoff A, Carrie A, Gelot A, Dupuis E, Motte J, Berwald-Netter Y, Catala M, Kahn A, Beldjord C, Chelly J (1998) A novel CNS gene required for neuronal migration and involved in X-linked subcortical laminar heterotopia and lissencephaly syndrome. Cell 92:51–61.

Edwards MA, Caviness VS Jr, Schneider GE (1986) Development of cell and fiber lamination in the mouse superior colliculus. J Comp Neurol 248:395–409.

Finlay BL, Berg AT, Sengelaub DR (1982) Cell death in the mammalian visual system during normal development: II. Superior colliculus. J Comp Neurol 204:318–324.

Gallyas F (1979) Silver staining of myelin by means of physical development. Neurol Res 1:203–209.

Gleeson JG, Allen KM, Fox JW, Lamperti ED, Berkovic S, Scheffer I, Cooper EC, Dobyns WB, Minnerath SR, Ross ME, Walsh CA (1998) Doublecortin, a brain-specific gene mutated in human X-linked lissencephaly and double cortex syndrome, encodes a putative signaling protein. Cell 92:63–72.

Gloster A, El-Bizri H, Bamji SX, Rogers D, Miller FD (1999) Early induction of Talpha1 alpha-tubulin transcription in neurons of the developing nervous system. J Comp Neurol 405:45–60.

Govek EE, Newey SE, Van Aelst L (2005) The role of the Rho GTPases in neuronal development. Genes Dev 19:1–49.

Groszer M, Erickson R, Scripture-Adams DD, Dougherty JD, Le Belle J, Zack JA, Geschwind DH, Liu X, Kornblum HI, Wu H (2006) PTEN negatively regulates neural stem cell self-renewal by modulating G0-G1 cell cycle entry. Proc Natl Acad Sci U S A 103: 111–116.

Guerrini R, Marini C (2006) Genetic malformations of cortical development. Exp Brain Res 173:322–333.

Hong SE, Shugart YY, Huang DT, Shahwan SA, Grant PE, Hourihane JO, Martin ND, Walsh CA (2000) Autosomal recessive lissencephaly with cerebellar hypoplasia is associated with human RELN mutations. Nat Genet 26:93–96.

Isaacs AM, Oliver PL, Jones EL, Jeans A, Potter A, Hovik BH, Nolan PM, Vizor L, Glenister P, Simon AK, Gray IC, Spurr NK, Brown SD, Hunter AJ, Davies KE (2003) A mutation in Af4 is predicted to cause cerebellar ataxia and cataracts in the robotic mouse. J Neurosci 23:1631–1637.

Keays DA, Cleak J, Huang GJ, Edwards A, Braun A, Treiber CD, Pidsley R, Flint J (2010) The role of Tuba1a in adult hippocampal neurogenesis and the formation of the dentate gyrus. Dev Neurosci 32:268–277.

Keays DA, Tian G, Poirier K, Huang GJ, Siebold C, Cleak J, Oliver PL, Fray M, Harvey RJ, Molnar Z, Pinon MC, Dear N, Valdar W, Brown SD, Davies KE, Rawlins JN, Cowan NJ, Nolan P, Chelly J, Flint J (2007) Mutations in alpha-tubulin cause abnormal neuronal migration in mice and lissencephaly in humans. Cell 128:45–57.

Koch M (1999) The neurobiology of startle. Prog Neurobiol 59: 107–128.

Lein ES, Hawrylycz MJ, Ao N, Ayres M, Bensinger A, Bernard A, Boe AF, Boguski MS, Brockway KS, Byrnes EJ, Chen L, Chen L, Chen TM, Chin MC, Chong J, Crook BE, Czaplinska A, Dang CN, Datta S, Dee NR, Desaki AL, Desta T, Diep E, Dolbeare TA, Donelan MJ, Dong HW, Dougherty JG, Duncan BJ, Ebbert AJ, Eichele G, Estin LK, Faber C, Facer BA, Fields R, Fischer SR, Fliss TP, Frensley C, Gates SN, Glattfelder KJ, Halverson KR, Hart MR, Hohmann JG, Howell MP, Jeung DP, Johnson RA, Karr PT, Kawal R, Kidney JM, Knapik RH, Kuan CL, Lake JH, Laramee AR, Larsen KD, Lau C, Lemon TA, Liang AJ, Liu Y, Luong LT, Michaels J, Morgan JJ, Morgan RJ, Mortrud MT, Mosqueda NF, Ng LL, Ng R, Orta GJ, Overly CC, Pak TH, Parry SE, Pathak SD, Pearson OC, Puchalski RB, Riley ZL, Rockett HR, Rowland SA, Royall JJ, Ruiz MJ, Sarno NR, Schaffnit K, Shapovalova NV, Sivisay T, Slaughterbeck CR, Smith SC, Smith KA, Smith BI, Sodt AJ, Stewart NN, Stumpf KR, Sunkin SM, Sutram M, Tam A, Teemer CD, Thaller C, Thompson CL, Varnam LR, Visel A, Whitlock RM, Wohnoutka PE, Wolkey CK, Wong VY, et al (2007) Genome-wide atlas of gene expression in the adult mouse brain. Nature 445:168–176.

Luo L (2000) Rho GTPases in neuronal morphogenesis. Nat Rev Neurosci 1:173–180.

Meloni EG, Davis M (1999) Muscimol in the deep layers of the superior colliculus/mesencephalic reticular formation blocks expression but not acquisition of fear-potentiated startle in rats. Behav Neurosci 113:1152–1160.

Meloni EG, Davis M (2000) GABA in the deep layers of the superior Colliculus/Mesencephalic reticular formation mediates the enhancement of startle by the dopamine D1 receptor agonist SKF 82958 in rats. J Neurosci 20:5374–5381.

Merry DE, Veis DJ, Hickey WF, Korsmeyer SJ (1994) bcl-2 protein expression is widespread in the developing nervous system and retained in the adult PNS. Development 120:301–311.

Morris-Rosendahl DJ, Najm J, Lachmeijer AM, Sztriha L, Martins M, Kuechler A, Haug V, Zeschnigk C, Martin P, Santos M, Vasconcelos C, Omran H, Kraus U, Van der Knaap MS, Schuierer G, Kutsche K, Uyanik G (2008) Refining the phenotype of alpha-1a Tubulin (TUBA1A) mutation in patients with classical lissencephaly. Clin Genet 74:425–433.

Park HJ, Kong JH, Kang YS, Park WM, Jeong SA, Park SM, Lim JK, Jeon CJ (2002) The distribution and morphology of calbindin D28K- and calretinin-immunoreactive neurons in the visual cortex of mouse. Mol Cells 14:143–149.

Paxinos G, Halliday GM, Watson C, Koutcherov Y, Wang H (2007) Atlas of the developing mouse brain. London: Academic Press.

Pistorio AL, Hendry SH, Wang X (2006) A modified technique for high-resolution staining of myelin. J Neurosci Methods 153: 135–146.

Porter AG, Janicke RU (1999) Emerging roles of caspase-3 in apoptosis. Cell Death Differ 6:99–104.

Sakakibara S, Misaki K, Terashima T (2003) Cytoarchitecture and fiber pattern of the superior colliculus are disrupted in the Shaking Rat Kawasaki. Brain Res Dev Brain Res 141:1–13.

Sanno H, Shen X, Kuru N, Bormuth I, Bobsin K, Gardner HA, Komljenovic D, Tarabykin V, Erzurumlu RS, Tucker KL (2010) Control of postnatal apoptosis in the neocortex by RhoA-subfamily GTPases determines neuronal density. J Neurosci 30:4221–4231.

Shammah-Lagnado SJ, Negrao N, Silva BA, Ricardo JA (1987) Afferent connections of the nuclei reticularis pontis oralis and caudalis: a horseradish peroxidase study in the rat. Neuroscience 20:961–989.

Tan SS, Valcanis H, Kalloniatis M, Harvey A (2002) Cellular dispersion patterns and phenotypes in the developing mouse superior colliculus. Dev Biol 241:117–131.

Tsunekawa N, Yanagawa Y, Obata K (2005) Development of GABAergic neurons from the ventricular zone in the superior colliculus of the mouse. Neurosci Res 51:243–251.

Vekrellis K, McCarthy MJ, Watson A, Whitfield J, Rubin LL, Ham J (1997) Bax promotes neuronal cell death and is downregulated during the development of the nervous system. Development 124:1239–1249.

Watakabe A, Ichinohe N, Ohsawa S, Hashikawa T, Komatsu Y, Rockland KS, Yamamori T (2007) Comparative analysis of layer-specific genes in Mammalian neocortex. Cereb Cortex 17:1918–1933.

Wittmann T, Waterman-Storer CM (2001) Cell motility: can Rho GTPases and microtubules point the way? J Cell Sci 114:3795–3803.

(Accepted 17 August 2011)
(Available online 22 August 2011)